Eur Biophys J (1996) 24: 233–242

European Biophysics Journal

Pigment-protein interactions in *Rhodobacter sphaeroides* Y photochemical reaction center; comparison with other reaction center structures

Bernadette Arnoux[1], **Françoise Reiss-Husson**[2]

[1] Laboratoire de Biologie Structurale, Bâtiment 34, C.N.R.S., Gif-sur-Yvette, France
[2] Centre de Génétique Moléculaire, Bâtiment 24, C.N.R.S., Gif-sur-Yvette, France

Received: 18 July 1995/Accepted in revised form: 22 January 1996

Abstract. Structural characteristics of pigments and cofactors are analyzed in the X-ray structure of the *Rhodobacter sphaeroides* (Y strain) photochemical reaction center, recently refined at 3 Å resolution (Arnoux B, Gaucher JF, Ducruix A and Reiss-Husson F (1995) Acta Cryst D51: 368–379). As several structures are now available for these pigment-protein complexes from various *Rhodobacter sphaeroides* strains and for *Rhodopseudomonas viridis,* a detailed comparison was done for highlighting converging structural results as well as for pointing to incidental differences. Comparison of mean plane orientations and distances, and also direct superposition of the pigment arrays, indicated that the best agreement between all the structures concerned the dimer and the bacteriopheophytin of the A branch. In the Y reaction center structure the pentacoordination of the Mg^{++} atoms of the bacteriochlorophylls, and the H bonding pattern of the porphyrin conjugated carbonyls are consistent with the better resolved *Rhodobacter sphaeroides* recently published structure (Ermler U, Fritzsch G, Buchanan SK and Michel H (1995) Structure 2:925–936). Discrepancies between the various *Rhodobacter sphaeroides* structures are larger for the quinones, particularly the secondary one. In the Y reaction center structure the phytyl and isoprenoid chains of the cofactors are defined and their local mobility was evaluated by analyzing the temperature factor and the density of neighbouring atoms. Significant differences were observed between the A and B branches, and, within each branch, from the dimer to the quinone molecules.

Key words: Bacterial reaction center – Crystal structure – Cofactor interactions – Structure comparison – Photosynthesis

Correspondence to: F. Reiss-Husson (Tel.: (33) 1 69 82 38 30, Fax: (33) 1 69 82 35 62, e-mail: freiss@cgm.cnrs-gif.fr)

Introduction

The resolution of the three-dimensional structure of photochemical reaction centers (RCs) from two purple photosynthetic bacteria (Deisenhofer et al. 1985a,b; Chang et al. 1986; Allen et al. 1986) has been a major breakthrough for membrane protein research. Long hydrophobic α helices are the dominant secondary structure elements of the RC subunits; this feature, probably common to a large class of integral membrane proteins, is a key factor for their modelling. Another property is the association of the RC with detergent molecules in the three-dimensional crystals (Roth et al. 1989, 1991); this accounts for the role of detergent in the solubilization and the crystallization of membrane proteins.

In the field of photosynthesis, the discovery of the RC structure allowed the investigation, at the molecular level, of the electron and proton transfers which are initiated by light excitation. It is now clear that these reactions not only depend on the electronic properties of the chromophores, but also on their relative orientations and distances, and on their proteic environment. These structural parameters are thus of prime importance for the interpretation of a variety of spectroscopic and genetic experiments (see Gunner 1991 for a review). For this purpose, the structures of the RCs from *Rhodopseudomonas (Rps.) viridis* (Deisenhofer et al. 1995) and from several *Rhodobacter (Rb.) sphaeroides* strains (Allen et al. 1987, 1988; Komiya et al. 1988; Yeates et al. 1988; Chang et al. 1991; El-Kabbani et al. 1991; Chirino et al. 1994; Ermler et al. 1994; Arnoux et al. 1995) are available and permit a detailed comparison (Table 1). The fold of their polypeptide backbone and the assembly of pigments can be superposed with a very good match. However, when the first sets of data concerning *Rb. sphaeroides* (4RCR, 2RCR) were compared to *Rps. viridis,* some controversies arose concerning interactions of chromophores with neighbouring residues (Komiya et al. 1988; El-Kabbani et al. 1991). Some of these differences were later reconsidered when refinement reached 3.0 Å, and when another refined data set (1PSS) became available (Chirino et al. 1994). Recently, a different crys-

Table 1. Reaction center structures

Bacterial strains	PDB code	Space group	Resolution limit [Å]	No. of unique reflections[a]	Completeness (%)	R-factor [%]	Mean coordinate error	B value ($Å^2$) averaged for all atoms	B value ($Å^2$) averaged for cofactors	Reference
Rps. viridis	1PRC	$P4_32_12$	2.3	95762	75.4	19.3	0.26	20.9[b]	15.9	Deisenhofer et al. 1995
Rb. sphaeroides										
R26	4RCR	$P2_12_12_1$	2.8	23349	62.0	22.7	0.4	30.4	25.0	Allen et al. 1988
R26	2RCR	$P2_12_12_1$	3.1	13493	59.0	22.0	0.5	9.0[c]	–	Chang et al. 1991
ATCC 17023[d]	1PSS	$P2_12_12_1$	3.0	18066	73.6	22.3	0.5	29.7	21.0	Chirino et al. 1994
ATCC 17023[d]	1PCR	$P3_121$	2.65	55036	88.9	18.6	0.3	34.5	43.0[e]	Ermler et al. 1994
Y[f]	1YST	$P2_12_12_1$	3.0	19630	80.0	22.9	0.4	39.6	30.0	Arnoux et al. 1995

[a] Used in the refinement
[b] Calculated for the L, M and H subunits and cofactors
[c] Individual B factors were not introduced in the refinement
[d] Also called 2.4.1
[e] This value is relatively high because of the temperature factor of Q_B, which is 80 $Å^2$
[f] Collection number: DSM 160

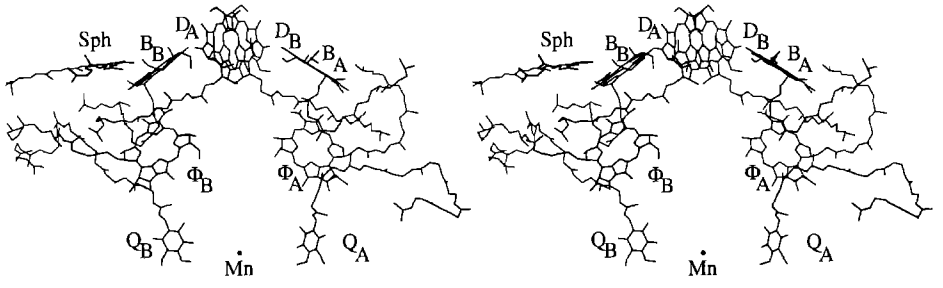

Fig. 1. Stereodiagram of a wire model of the cofactor assembly in the 1YST structure with the pigment nomenclature

tal form diffracting at 2.65 Å resolution was obtained (Buchanan et al. 1993); its refined structure (1PRC) allowed clarification of the issue and stressed similarities between *Rb. sphaeroides* and *Rps. viridis* with regard to pigment/protein interactions (Ermler et al. 1994).

At the same time Arnoux et al. (1995) described the structure of the RC of another *Rb. sphaeroides* strain (Y) refined at 3.0 Å (1YST); interactions between subunits were analyzed and also particular features of this RC, which contains a manganese atom (instead of iron) interacting with the quinones and a 15–15′ cis-spheroidene in close contact with the monomeric bacteriochlorophyll of the B branch (Arnoux et al 1995). Here we report on the organization and the environment of the pigment array, including the phytyl and isoprenoid chains, and we compare our results with existing data. Because of the limited resolutions of *Rb. sphaeroides* RC structures, which are still in the medium range even for the best crystals, such comparison might help for distinguishing between real and incidental differences. Furthermore, within each data set, all chromophores are not described with the same precision. In *Rps. viridis* 1PRC which is the highest resolution structure (Table 1), the carotenoid and the secondary quinone have an electron density which is poorly defined (Deisenhofer et al. 1995). In the best *Rb. sphaeroides* crystals (1PCR), the secondary quinone is only partly present (Ermler et al. 1994), while its occupancy is much higher in the 1YST crystals (Reiss-Husson et al. 1990) and the 2RCR and 4RCR ones.

Experimental

Pigment nomenclature. In this paper we used for the pigments the nomenclature which is now generally adopted for bacterial RCs (see Fig. 1), where the subscript (A or B) indicates the pigment branch; D_A and D_B are the bacteriochlorophyll (Bchl) molecules of the dimer, B_A and B_B the monomeric Bchls, Φ_A and Φ_B the bacteriopheophytins (Bpheo), Q_A and Q_B the quinone molecules.

Structure comparisons. For an easier comparison of all RC structures, the different sets of coordinates were superimposed by a least-squares procedure using the Mg^{++} atoms of the Bchls and the metal ion (Mn or Fe) as reference points. With this procedure the rms deviation on the α carbons of the eleven transmembrane helices is 0.9±0.1 Å. If the α carbons of these helices are used as reference points the rms deviations are in the same range.

Mean planes and distances between planes. Each porphyrin plane was defined by the nitrogen and carbon conju-

gated atoms. The SHELXL93 program (Sheldrick 1993) was used to calculate mean plane equation and angles between these planes. Distances between planes were measured beween Mg^{++} atoms for Bchls, centre of nitrogen atoms for Bpheos and centre of cycle carbon atoms for the quinones.

Neighbour density around phytyl or isoprenoid chains was calculated for each carbon atom as follows: a sphere of 8 Å radius was centered on the C atom and the atoms located within this sphere were numbered (N in Fig. 6).

Results

Cofactor assembly

The spatial arrangement of the pigments and cofactors in 1YST (Fig. 1) is characterized by a pseudo twofold axis relating the porphyrin rings of the dimer Bchl molecules (D_A and D_B), the monomeric Bchl molecules (B_A and B_B), the Bpheo molecules (Φ_A and Φ_B) and the quinone cycles of Q_A and Q_B. This axis, which crosses the manganese atom and defines two pigment branches A and B, also relates the backbone of the L and M subunits. This pseudo symmetry is broken by a 15–15′-cis spheroidene, which is located near B_B (Arnoux et al. 1989, 1995), by some of the phytyl chains of the Bchls and Bpheos, and by isoprenoid tails of the quinones. In the 1YST X-ray structure, the porphyrin rings are precisely defined in the electron density on both pigment branches; the phytyl chains and the isoprenoid tails of the quinones could be traced almost completely although their thermal factors are generally larger, as discussed below. A weak departure from a perfect twofold symmetry is observed for the porphyrin planes between the A and B pigment branches: the best superposition is observed with a 177.2°, 172.2° and 173.5° rotation for the dimer, the monomeric Bchls and the Bpheos respectively. These values are in excellent agreement with those determined in 1PCR (Ermler et al. 1994).

For comparing macrocycles, mean planes were defined by the atomic coordinates of the porphyrin and quinone rings. The deviations of the porphyrin ring atoms from the mean plane are quite small for the dimer and the monomeric Bchls (average rms deviation at most 0.07 Å). Slightly higher deviations are found for the Bpheos (0.16 Å). This is in contrast with 1PCR structure, where a significant puckering of D_A was observed at ring V, but where pheophytin rings were more planar (Ermler et al 1994).

For a more precise comparison the angles between these mean planes and the center-to-center distances of the cofactor cycles were determined in 1YST and compared to values calculated in the same way for the other RC structures (Table 2 and Fig. 2). The relative orientation of the Bchl dimer molecules in 1YST is in best agreement with the 1 PCR structure. One may note that this D_AD_B angle fluctuates in the various *Rb. sphaeroides* structures within a range of values distinctly lower than the value for *Rps. viridis*. This difference is reliable, as in each data set the dimer is certainly the part for which the electron density

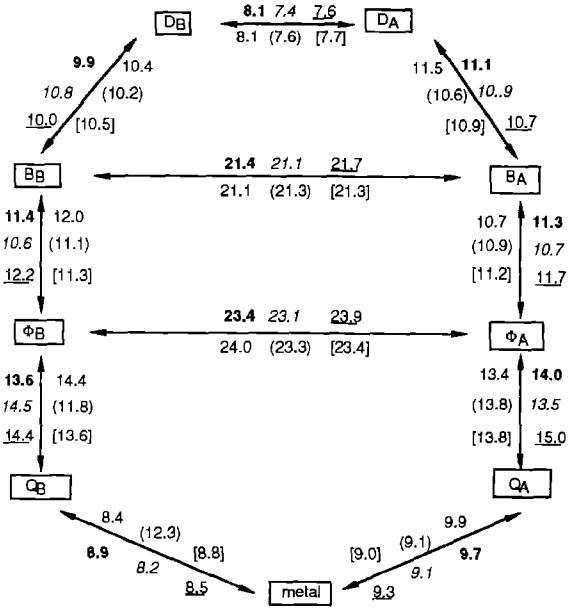

Fig. 2. Distances between centers of pigments or quinone cycles in the various RC structures. Codes are the following: bold: 1YST. Italics: 1PRC. Standard: 4RCR. Brackets: 1PCR. Square brackets: 1PSS. Underlined: 2RCR

Table 2. Angles between mean planes (°) for pigments, cofactors and some residues. Values in brackets are less precise because of low Q_B occupancy

	Rb. sphaeroides					*Rps. viridis*
	1YST	1PSS	4RCR	2RCR	1PCR	1PRC
D_A/D_B	6.7	9.8	8.5	8.0	6.8	11.8
D_A/B_A	64.5	62.9	62.8	63.7	65.5	64.1
D_B/B_B	67.1	66.0	66.1	66.6	61.2	71.9
B_A/Φ_A	59.9	68.1	69.0	67.2	67.5	63.3
B_B/Φ_B	60.2	63.7	66.2	61.4	68.0	58.3
Φ_A/Q_A	39.6	32.5	40.0	54.6	34.2	38.5
Φ_B/Q_B	34.0	39.9	36.1	32.5	(28.7)	(58.7)
Q_A/Q_B	28.3	34.1	29.0	56.8	(9.4)	(42.5)
Q_A/TrpM252	44.0	33.0	46.9	27.3	15.5	44.6
Q_B/PheL216	6.0	78.7	68.4	22.1	(31.4)	13.2

is the best defined. It is the only notable difference between the two purple bacteria as regards the relative orientations of the mean porphyrin planes. The shortest distance between porphyrin cycles is observed for the pyrrole rings I of the dimer, which is 3.7 Å (C1–C1) in 1YST and 3.4 Å in 1PCR (Ermler et al. 1994). When the distances between geometrical centers of cofactor cycles (Fig. 2) of the 4 Bchls are compared, values found in the various structures lie within a rather narrow range ($\sigma \leq 0.3$ Å). Distances between monomeric Bchls and Bpheos are slightly more scattered, particularly on the B branch.

The plane of the quinone ring of Q_A is oriented relative to the Φ_A plane in the same way for all RC structures, and distances between Φ_A and Q_A centers agree well (13.7 Å, $\sigma \leq 0.5$ Å) (Table 2) if one excepts the 2RCR structure for

which the Q_A position is different (Fig. 4). The tilt angles of the Q_B plane towards both the Φ_B and Q_A planes are also in good agreement in the 1YST, 1PSS and 4RCR structures. In these structures the distances between the Φ_B and Q_B centers, as well as between the quinones and the metal, also lie within a narrow range ($\sigma \leq 0.4$ Å). Values for the Q_B orientation and position in 1PCR and in *Rps. viridis* differ from the other structures; however, because of the very low occupancy of Q_B in these crystals they are less reliable.

One may note that in all structures, except 1PCR, Q_B is closer to the metal ion than Q_A, irrespective of the nature of the metal (Mn^{++} in YRC, Fe^{++} in the others).

Interactions between cofactor cycles and residues and comparison with other RC structures

As already discussed (Arnoux et al. 1995), the protein backbone of the YRC is highly homologous to those of other *Rb. sphaeroides*. However, analysis of interactions between aminoacids and cofactors reveals larger discrepancies between the various structures than for the geometry of the pigment assembly. Discrete residue side chains are indeed not always in the same conformation.

Mg^{++} ligand of the 4 Bchls. In 1YST, the fifth Mg^{++} ligand of the Bchls, which is His residue, superimposes best with homologous ones of the 1PCR structure. These Mg^{++}-histidine distances (Table 3) are quite comparable to those found in the *Rps. viridis* structure, and also in the high resolution structure of the soluble Bchl-protein complex from *Prosthecochloris aestuarii* (Tronrud et al. 1986). The differences observed in the other structures (2RCR, 4RCR and 1PSS) (Chirino et al. 1994) for some of the Mg^{++}-histidine distances probably stem from the medium resolution.

Dimer. In 1YST the interactions between the protein and each of the Bchl molecules of the dimer are of different type (Table 3): only van der Waals contacts with hydrophobic residues are observed for D_B, whereas two H bonds are observed for D_A, concerning respectively ring V carbonyl CO and Cys L247 Sγ, and ring I acetyl CO and His L168 Nε_2. The Nδ_2 atom of His L168 is H bonded to Leu M183 carbonyl and to Asn L166 Oδ_1 (Arnoux et al. 1995), as in all other *Rb. sphaeroides* structures, except the 2RCR one. His L168 is an H bond donor in all RC structures, whereas Cys L247 is only implicated in 1YST and 1PSS structures. It may be noted that in *Rps. viridis* a glycine is found at L247 instead of a cysteine.

Table 3. Distances between selected residues and cofactors

			1YST	4RCR	2RCR	1PSS	1PCR		1PCR	
D_A	Mg^{++}	HisL173 Nε_2	2.2	2.7	3.2	2.3	2.3	Mg^{++}	HisL173 Nε_2	2.2
	Acetyl I	HisL168 Nε_2	3.5	3.6	2.6	2.5	3.2	Acetyl I	HisL168 Nε_2	2.8
	Keto V	(MetL248 Sδ)						Keto V	ThrL248 Oγ	2.6
	Carbonyl V	(MetL248 Sδ)						Carbonyl V	ThrL248 Oγ	3.5
	Carbonyl V	CysL247 Sγ	3.5	4.2	>5	3.3	3.7	Carbonyl V	(GlyL247)	
D_B	Mg^{++}	HisM202 Nε_2	2.3	2.0	2.3	2.1	2.2	Mg^{++}	HisM202 Nε_2	1.9
	Acetyl I	(PheM197)						Acetyl I	TyrM195 OH	3.0
B_A	Mg^{++}	HisL153 Nε_2	2.3	4.5	3.0	2.8	2.3	Mg^{++}	HisL153 Nε_2	2.2
	Keto V						water	Keto V	water	
B_B	Mg^{++}	HisM182 Nε_2	2.3	1.9	2.2	2.0	2.2	Mg^{++}	HisM180 Nε_2	2.1
	Carbonyl IV	SerL178 Oγ	2.9	3.4	3.1	>5	>5	Carbonyl IV	SerL178 Oγ	3.6
Φ_A	Carbonyl V	TrpL100 Nε_1	3.2	3.8	3.1	2.9	2.9	Carbonyl V	TrpL100 Nε_2	3.0
	Keto V	GluL104 Oε_1	2.7	2.9	3.1	2.7	2.7	Keto V	GluL104 Oε_1	2.7
Φ_B	Carbonyl V	TrpM129 Nε_1	3.2	2.9	3.0	2.8	2.8	Carbonyl V	TrpM129 Nε_1	2.7
Q_A	O2	HisM219 Nδ_1	4.6	4.5	4.8	3.3	3.2	O2	HisM219 Nδ_1	3.1
	O2	ThrM222 Oγ	3.1	2.8	2.4	3.8	3.6	O2	ThrM220 Oγ	3.6
	O2	TrpM252 Nε_1	3.8	3.3	4.6	4.2	4.4	O2	TrpM250 Nε_1	4.1
	O5	AlaM260 N	2.8	2.7	2.5	2.6	2.8	O5	AlaM258 N	3.1
	Methoxy O4	AlaM260 N	2.6	4.5	>5	3.9	3.6	–	–	
	Methoxy O4	ThrM261 N	3.4	4.5	3.8	4.7	>5	–	–	
Q_B	O2	HisL190 Nδ_1	2.7	2.6	2.9	2.8	>3.5	O2	HisL190 Nδ_1	2.7
	O2	IleL224 N	>5	>5	>5	>5	2.8	O2	IleL224 N	>5
	O5	SerL223 Oγ	>5	2.7	3.0	3.4	>3.5	O5	SerL223 Oγ	2.7
	O5	IleL224 N	3.5	3.2	>5	3.0	>5	O5	IleL224 N	3.2
	O5							O5	GlyL225 N	2.7
	Methoxy O4	SerL223 Oγ	4.2	>5	>5	3.1	>5	O4		
	Methoxy O4	ThrL226 N	>5	3.4	>5	4.9	>5	O4	AlaL226 N	2.9
	Methoxy O4	IleL224 N	3.4	>5	>5	4.5	>5	O4		
	Methoxy O3	GluL212 Oε_1	3.2	3.2	2.9	3.8	water	O3	HisL190 Nδ_1	3.0
	Methoxy O3	IleL224 N	>5	>5	>5	>5	2.9	O3	IleL224 N	>5

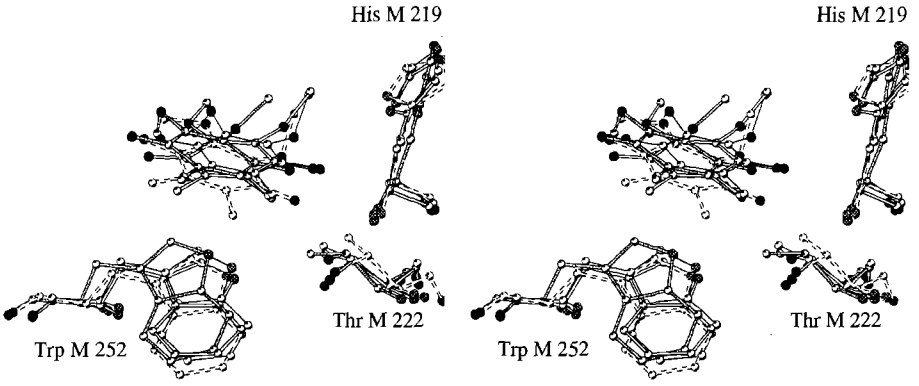

Fig. 3. Stereodiagram of the superposition of several *Rb. sphaeroides* structures showing the quinone Q_A cycle, and selected neighbouring residues (His M219, Thr M222, TrpM252). Symbols are the same as in Fig. 4

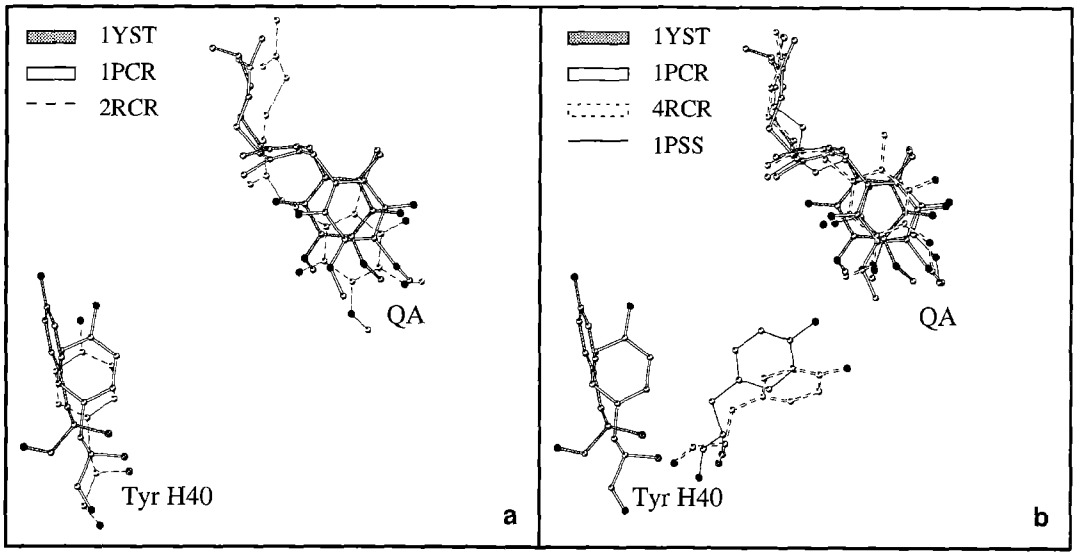

Fig. 4a,b. Superposition of several *Rb. sphaeroides* structures showing the quinone Q_A cycle and Tyr H40 in: **a** 1YST, 1PCR and 2RCR **b** 1YST, 4RCR, 1PSS and 1PCR

The absence of H bonds on D_B in all *Rb. sphaeroides* structures contrasts with *Rps. viridis,* where the D_B acetyl CO is H bonded to Tyr M195 (homologous to Phe M197 in *Rb. sphaeroides*).

Monomeric Bchls. In the 1YSt structure there is no H bond found for B_A, and only one occurs for B_B between the propionic carbonyl of cycle IV and Ser L178 Oγ (Table 3). When the position of this residue is analyzed in the other RC structures two alternative orientations are found: either closer to cycle IV (in 2RCR, 4RCR, 1YST and 1PRC), or to cycle V (in 1PSS and 1PCR), which explains the differences reported in Table 3. The keto group of B_A, considered to be free of H bonds in 2RCR, 4RCR, 1PSS and 1YST, has been shown to interact with a water molecule in the higher resolution structures 1PRC and 1PCR.

Spheroidene. This carotenoid is bound as a 15–15′ isomer in 1YST. The shortest distance between spheroidene atoms and another pigment occurs between C15′ and the acetyl O atom of the B_B ring I (2.9 Å). The central position of the cis bond is in accordance with the electron density map (Arnoux et al. 1995) and also with resonance Raman (Arnoux et al. 1989) and NMR (De Groot et al. 1992) spectroscopic data. Spheroidene is surrounded by residues of the M subunit, mainly localized in the A, B, C helices and in the loop between the C and CD helices. It is buried in a hydrophobic cavity lined by bulky residues: 5 Trp and 9 Phe are closer than 5 Å. The C2–C5 end of the molecule is inserted between the parallel aromatic rings of Phe M123 and Phe M162.

One may wonder why spheroidene is localized in an hydrophobic pocket with the M subunit of the RC, as another pocket defined on the L subunit by the pseudo-twofold symmetry is even wider. However, the center of the latter cavity, corresponding to the position of the cis bond of the putative carotenoid, is obstructed by Phe L146, while in the true binding site the homologous residue (Val M175) allows enough space for the pigment cis bond.

It should be noted that two other conformations have been modeled for this pigment in 1PCR and 1PSS; they however could not be reconciled with spectroscopic properties.

Bpheophytins. In the whole set of structures, with the exception of 4RCR, a very good agreement is observed for the binding interactions of Φ_A and Φ_B with neighbouring residues (Table 3). The asymmetric distribution of H bond-

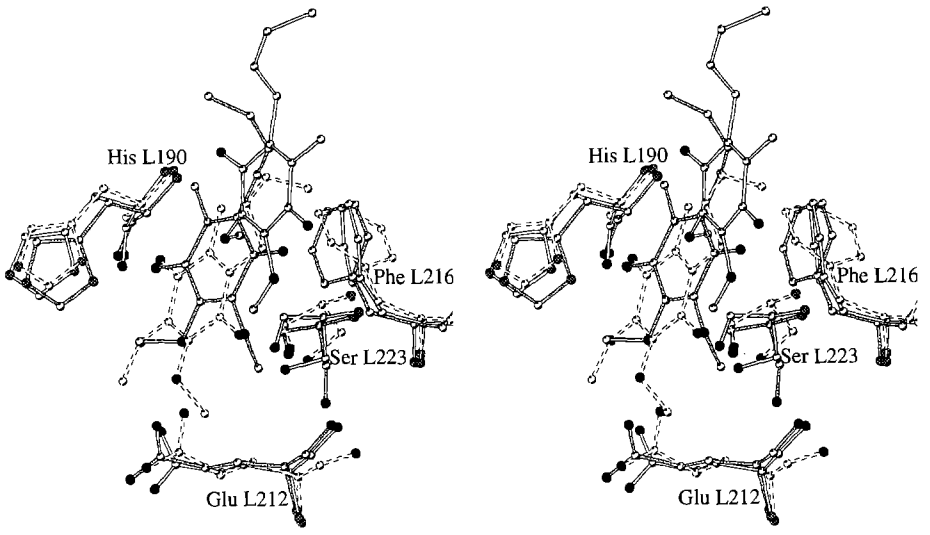

Fig. 5. Stereodiagram of the superposition of *Rb. sphaeroides* 1YST, 4RCR and 1PCR structures showing the Q_B cycle, and selected residues: His L190, Ser L223, Phe L216 and Glu L212. Same symbols as in Fig. 4

ing of the cycle V keto carbonyls of Φ_A and Φ_B is a common feature extending to *Rps. viridis*, as well as the symmetrical bonding of the methoxy carbonyls and Trp residues of the L and M subunits respectively.

Primary quinone Q_A. The binding pocket of the Q_A cycle is characterized by a pronounced hydrophobicity; only one charged group (Glu M234) is at less than 8 Å from a Q_A cycle atom (CM3). Both quinonic oxygens of Q_A are H bonded to residues of the M subunit in the 1YST structure as in all the other ones (Table 3). The shortest H bond distance is reproducibly observed for O5 and Ala M260 N in *Rb. sphaeroides* RC structures. On the other hand, results diverge for the hydrogen bond donor to O2: Thr M222 in the 1YST and 2RCR structures, His M219 in 1PSS and 1PCR (and in *Rps. viridis*), Thr M222 and Trp M252 in 4RCR. Furthermore one of the methoxy oxygens (O4) is at H bonding distance from peptide N atoms of residues M260 and M261 only in the 1YST structure.

These differences stem from the positions and orientations of these side chains and also of the quinone cycle (Figs. 3–4). Thus in the 1YST structure the rotation of His M219 around the $C\beta$–$C\gamma$ bond (as compared to the other structures) explains the increased distance of this residue to quinone O2 (Fig. 3). Even if the orientations of the Q_A cycle are not strictly the same, the position of the quinone O2 atom itself is only slightly different in the various structures, with the exception of the 2RCR one (Fig. 4).

Trp M252 has been pinpointed as occupying a remarkable position between Q_A and Φ_A in *Rps. viridis* and *Rb. sphaeroides* RCs (Stilz et al. 1994). Indeed it is similarly positioned in all RC structures (Fig. 3). Nevertheless the orientations of its aromatic part are diverse, being nearly parallel to the Q_A cycle only in 1PCR (Fig. 3 and Table 2) and in *Rps. viridis* 1PRC. As a consequence different H bonding patterns are also observed for this residue.

A general agreement is observed for the Q_A environment with the notable exception of Tyr H40. In 1PSS and 4RCR this residue is located towards the Q_A cycle and its hydroxyl group is close to one of the Q_A methoxy groups (Fig. 4a). In all other structures, including *Rps. viridis*, Tyr H40 is quite distant from the Q_A cycle (Fig. 4b): e.g. in 1YST the closest distance between Tyr H40 oxygen and Q_A is 11.6 Å, while this residue is in contact with the extremity of the Q_A isoprenoid chain.

Metal ion. In 1YST Mn^{++} is hexa-coordinated to the $N\varepsilon_2$ atoms of His L190, His L230, His M219 and His M266, and to $O\varepsilon_1$ and $O\varepsilon_2$ atoms of Glu M234. These ligands are the same as those of Fe^{++} in the other RCs; the metal/ligand distances are in excellent agreement with 1PCR and 1PRC (Arnoux et al. 1995).

Secondary quinone Q_B. This quinone is located in a much more polar environment than Q_A: in 1YST 3 acidic groups (Glu L212 and M234, and Asp L213) are found at less than 6 Å from Q_B cycle atoms; Glu L212 could be an H bond donor for one of the methoxy oxygens (O3). The shortest H bond is observed for O2 oxygen and His L190 $N\delta_1$, whose $N\varepsilon_2$ is a ligand of the Mn^{++} atom (Arnoux et al. 1995). For the other quinonic oxygen (O5) a possible H bond donor could be the peptide N of Ile L224, which is also at H bonding distance from the other methoxy oxygen (O4).

When these data are compared to the other orthorhombic structures (Table 3), an excellent agreement is found for the interactions between O2 and His L190, but not for O5 oxygen and neighbouring residues. In the 2RCR, 4RCR and 1PSS structures, O5 is at hydrogen bonding distances from Ser L223 $O\gamma$, and also (in 4RCR and 1PSS) from the peptide N of Ile L224. Only the latter H bond might occur in 1YST; the Ser L223 side chain is rotated and its hydroxyl is engaged in a H bond with Asp L213 (Fig. 5).

A quite different picture emerges when the localization of Q_B in the 1PCR structure is analyzed. The quinone cycle is displaced and rotated in such a way that O2 is now H bonded to the peptide N of Ile L224, and O5 is free of interaction with the protein. This position of Q_B is not presently explained as the folding of the binding pocket itself is comparable in all structures; it has been attributed to the different redox state of Q_B (presumed to be a quinol) in these crystals. Because of the high temperature factor and

the poor quality of the electron density the position of Q_B in these crystals is only tentative (Ermler et al 1994).

In the 1YST structure, the aromatic ring of Phe L216 is quite parallel to the Q_B cycle (Fig. 5 and Table 3), as also observed in *Rps. viridis* RC (Deisenhofer et al. 1995). This stacking interaction is not observed in the other *Rb. sphaeroides* structures.

Interactions between phytyl or isoprenoid chains and residues

In the 1YST structure the phytyl and isoprenoid chains of the cofactors are almost completely defined in the electron density (Arnoux et al. 1995). Thus we could determine their possible mobility by considering their thermal factors and the density of atoms located nearby (belonging either to residues or to other pigments).

For the dimer Bchl molecules, and only for them, the pseudo twofold symmetry relating the porphyrin cycles also governs the structure of the phytyl chains. The chains of the dimer are closely surrounded by hydrophobic residues up to their C10 atom, then neighbours are scarce (Fig. 6). The density of neighbours (as defined in Experimental) along the phytyl chains of B_A and B_B decreases similarly, but on average are lower than for the dimer chains. A quite different pattern is observed for the Bpheos. The Φ_A chain (Fig. 6) is heavily surrounded by residues along its whole length at the difference of Φ_B one. It is interesting to note that the last carbon atom of Φ_A is in close contact with B_A ring I and at short distance from Phe L146. This residue has already been implicated in blocking the occupation by a carotenoid of a pseudo binding site on the A branch (Arnoux et al. 1990). The end of Φ_A phytyl chain apparently plays the same role. On the B branch, neighbour density diminishes steadily along the Φ_B chain (Fig. 6); its extremity is protruding at the surface of the protein and exposed to the β octylglucoside molecules of the detergent belt. The weakness of this neighbour density implies a larger pocket around the Φ_B tail.

The neighbour density around Q_A and Q_B isoprenoid chains (Fig. 6) decreases abruptly from the first carbon atom (C7) till respectively the third or the fourth isoprenoid unit, and then reaches the lowest values as compared to the other cofactors. The poorer definition of these isoprenoid tails, except for their first unit, is related to their high thermal factors (Fig. 6).

The B factors of the Bpheos and of the monomeric Bchls are lower on the A branch than on the B branch; this might be correlated with the departure from the twofold symmetry observed for these chains (see Discussion). A contrario the strict symmetry governing the phytyl chain of the dimer results in equivalent B factors for D_A and D_B. In both pigment branches a regular decrease of the average thermal factor is otherwise observed from the quinone to the dimer (Fig. 6).

When the folding of these phytyl chains are compared in all RC structures, a remarkable superposition of the chains is observed for the dimer, B_A and Φ_A. The phytyl chain of B_B is not completely defined in 1PSS and 4RCR; the same folding as in 1YST is observed for 1PCR and 1PRC but not for 2RCR. Diverse foldings are observed for the Φ_B chain, when this chain is defined, owing to its looser contacts with residues. For the quinones, the poorer definition of their isoprenoid tails, except for their first units, explains why they were not completely defined in some of the other structures.

Discussion

In the present work we have analyzed the interactions within the pigments and cofactor assembly in Y *Rb. sphaeroides* RC, based on the three-dimensional structure at 3 Å resolution, and we have compared these results to several RC structures determined previously for other strains of the same species. Such a comparison is feasible as strain-to-strain differences are only few: primary sequences of these RCs are the same (except for one residue in Y RC (Arnoux et al 1990)); the presence of spheroidene in Y and ATCC 17023 strains or its absence in R26 strain does not perturb the other pigments; substitution of Fe by Mn in the Y strain does not modify the metal binding site. For some of these comparisons we also considered the *Rps. viridis* RC structure which is currently the most accurate one.

We first analyzed the general organization of the pigments and quinone cycles in terms of distances and relative orientations. For these calculations we considered mean porphyrin planes defined by the coordinates of all pyrrole N and conjugated C atoms. Indeed the resolution is unsufficient for assessing any significant puckering of these cycles in 1YST as in 2RCR, 4RCR, and 1PSS structures. A non planar deformation of the dimer molecules was only discussed for the better resolved 1PCR and 1PCR structures (Ermler et al 1994; Deisenhofer et al. 1995); however it might be influenced by the choice of force fields and topology parameters used for the refinement. The relative orientations of the mean dimer planes in 1YST and in 1PCR are almost equivalent. When comparing all *Rb. sphaeroides* structures to the *Rps. viridis* one a noteworthy difference is observed for this D_AD_B angle, which is markedly smaller in *Rb. sphaeroides*. This difference does not depend on the choice of atoms used to calculate the mean planes, being even larger if only pyrrole N are considered. It does not extend to the closest spacing between Bchl molecules of the dimer, which is similar in both bacterial species.

Comparison of mean plane orientations and distances, and also direct superposition of the pigment arrays, indicated that the best agreement between all the structures concerned the dimer and the Bpheo of the A branch. These molecules are functionally coupled in very fast reactions requiring tight relative positioning of the porphyrin cycles, indicated otherwise by low thermal factors. But it is remarkable that this agreement extends to their whole phytyl chains which present the same fold in all structures, despite the generally lower definition of the Φ_A chain. It may be noted that the curved shape of the Φ_A chain brings its terminus in close contact with the monomeric B_A cycle; on the B branch when the carotenoid is present near B_B the phytyl chain of Φ_B is constrained to another fold.

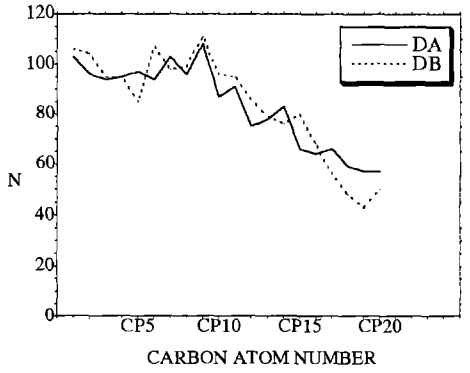

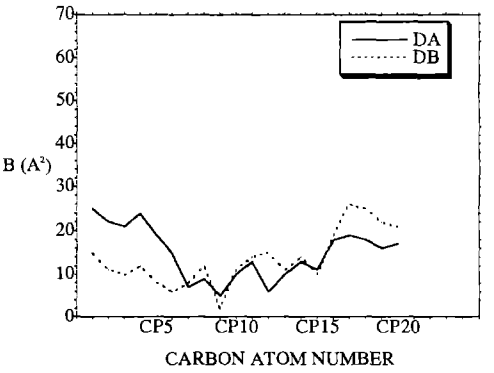

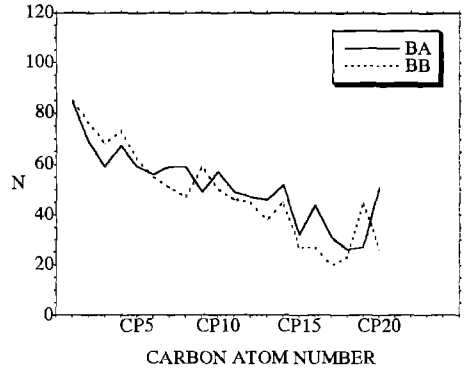

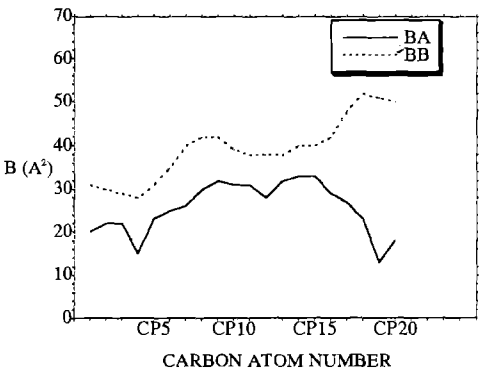

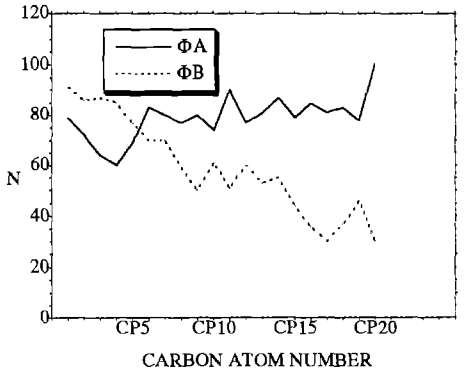

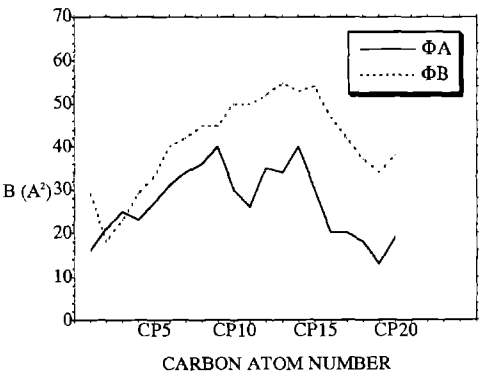

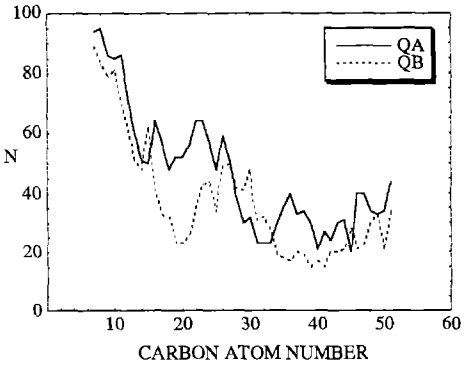

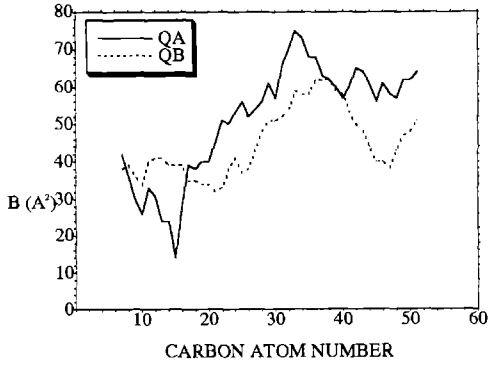

Fig. 6. Structural parameters of the phytyl or isoprenoid chains for the various cofactors in 1YST: density of neighbouring atoms (N, see experimental section) and isotropic thermal factor (B) for the carbon atoms of the chains. These 2 parameters are plotted as a fu tion of the position of the carbon atom in the chain

Ligand and polar interactions of the Bchl and Bpheo pigments with neighbouring residues in 1YST are generally consistent with those described in the better resolved 1PCR structure. The only divergence between 1YST and 1PCR lies in the polar interaction of B_A with SerL178, because of another conformation of this side chain in 1YST. Consequently our results confirm the structural similarities already stressed between *Rb. sphaeroides* and *Rps. viridis* RCs (Ermler et al. 1994; Arnoux et al. 1995), which concern the pentacoordination of the Mg^{++} atoms of the Bchls, and the H bonding pattern of the porphyrin conjugated carbonyls.

In all *Rb. sphaeroides* structures including 1YST both Q_A oxygens have polar interactions with neighbouring residues, and the shorter bond length is for O5 with peptide N of Ala M260. The position and orientation of the Q_A cycle in 1YST is in good agreement with other *Rb. sphaeroides* structures, except for 2RCR, even if the H bonding pattern of Q_A O2 is not strictly the same. Slight displacements both of the quinone and of neighbouring residues could not be avoided at medium resolution, and in our opinion explain these discrepancies.

For the quinone Q_B a valid comparison is restricted to *Rb. sphaeroides* 4RCR, 2RCR, 1PSS and 1YST, as the low Q_B content in crystals used for 1PCR and 1PRC structures decreased the corresponding electron density. The former four structures conclusively show that Q_B is closer to the metal ion than Q_A. Q_B localization is slightly different in 1YST, 1PSS, 2RCR and 4RCR in spite of a good occupancy, probably because of the inherent mobility of the secondary quinone indicated by its temperature factor. These various positions put a limit for the cavity offered to the Q_B cycle. Again various patterns are observed for some of the polar interactions of quinone oxygens with residues, and for stacking interactions of the quinone cycle. In 1YST Ser L223, which is considered to be the first proton donor for QH_2 formation (Paddock et al. 1990), is not H bonded to Q_B O5 but rather is engaged in polar interactions with Asp L213, unlike in the other structures. Glu L212, which is probably protonated and implicated as a donor for the second proton (Paddock et al. 1989), has polar interactions with one of the methoxy atoms in 1YST, 4RCR and 2RCR but not in 1PSS. These differences are probably incidental.

A word of caution is necessary when slight differences between these RC structures are discussed because of the possible influence of the isolation and crystallization conditions of the RC. Indeed the detergent used (either β octylglucoside or dodecyldimethylamine oxide), and also the crystallizing agents and additives differ. As a matter of fact, only the crystallization conditions of Y RC (Ducruix and Reiss-Husson 1987) do not involve addition of small amphiphiles (heptanetriol, benzamidine, or dioxane) used at high molarities for other RCs. It is not known if the presence of these small molecules during crystallization is totally innocuous for the most mobile part of the RC, that is for Q_B. Such "environmental" effects have indeed been observed for T7 RNA polymerase (Sousa et al. 1991); they could perhaps explain the displacement of Q_B in the 1PCR structure (Ermler et al. 1994).

The density of neighbouring atoms around the phytyl and isoprenoid chains in 1YST decreases regularly with the carbon number of the chain (except for Φ_A, see below), but with a slope which is the smallest for the dimer and the highest for the quinones. If the A and B branches are compared, equivalent variations are found for each couple of cofactors, except for Φ_A and Φ_B. The Φ_A chain is indeed densely surrounded by residue and pigment atoms till its end which comes into contact with the B_A cycle and hydrophobic residues; in contrast, the end of the Φ_B chain is exposed to the hydrophobic surface within the detergent belt. The variation of the B factors with the carbon atom number within a phytyl chain could be correlated with two parameters: the density and the thermal factor of their neighbours. The dimer chains are the most densely surrounded by atoms which present low B factors; hence the B factors of the dimer chains are both relatively constant and low. The environments of B_A and B_B chains are not symmetrical, in spite of an equivalent density of neighbours. The high thermal factor of the B_B chain, specially at its end, corresponds to those of surrounding atoms which belong mainly to the Q_B isoprenoid chain. The B_A chain is instead delineated with atoms with moderate B factors, especially at its end. The thermal factors of Φ_A and Φ_B chains are strongly correlated with their neighbour densities, as discussed above.

The density of neighbours along the isoprenoid chains of Q_A and Q_B is highest along the first three isoprenoid units; then it decreases to values which are the lowest of all chains. A direct correlation with B factor variations is observed: the lower the densities, the higher the B values. The tightness of the pocket around the first three isoprenoid units was already noted when the specificity of Q_A and Q_B binding versus length and nature of hydrophobic quinone tail was demonstrated (Warncke et al 1994). The binding pocket of the tail is not markedly wider for Q_B than for Q_A, in spite of the different binding constants of these quinones. The latter may rather be attributed to the different affinities of the quinone cycles towards their proteic surrounding.

Acknowledgements. We thank Dr. A. Ducruix for his constant interest and advice during this work. We also thank Dr. I. Agalidis and Dr. P. Sebban for useful suggestions and for reviewing the manuscript.

References

Allen JP, Feher G, Yeates TO, Rees DC, Deisenhofer J, Michel H, Huber R (1986) Structural homology of reaction centers from *Rhodopseudomonas sphaeroides* and *Rhodopseudomonas viridis* as determined by X-ray diffraction. Proc Natl Acad Sci USA 83:8589–8593

Allen JP, Feher G, Yeates TO, Komiya H, Rees DC (1987) Structure of the reaction center from *Rhodobacter sphaeroides* R-26: the cofactors. Proc Natl Acad Sci USA 84:5730–5734

Allen JP, Feher G, Yeates TO, Komiya H, Rees CD (1988) Structure of the reaction center from *Rhodobacter sphaeroides* R-26: protein-cofactor (quinones and Fe^{2+}) interactions. Proc Natl Acad Sci USA 85:8487–8491

Arnoux B, Ducruix A, Reiss-Husson F, Lutz M, Norris J, Schiffer M, Chang CH (1989) Structure of spheroidene in the photosyn-

thetic reaction center from Y *Rhodobacter sphaeroides*. FEBS Letters 58:47–50

Arnoux B, Ducruix A, Astier C, Picaud M, Roth M, Reiss-Husson F (1990) Towards the understanding of the function of *Rb. phaeroides* Y wild type reaction center: gene cloning, protein and detergent structures in the three dimensional crystals. Biochimie 72:525–530

Arnoux B, Gaucher JF, Ducruix A, Reiss-Husson F (1995) Structure of the photochemical reaction center of a spheroidene-containing purple bacterium, *Rhodobacter sphaeroides* Y, at 3 Å resolution. Acta Crystallogr D51:368–379

Buchanan SK, Fritzsch G, Ermler U, Michel H (1993) New crystal form of the photosynthetic reaction centre from *Rhodobacter sphaeroides* of improved diffraction quality. J Mol Biol 230:1311–1314

Chang CH, Tiede D, Tang J, Smith U, Norris J, Schiffer M (1986) Structure of *Rhodopseudomonas sphaeroides* R-26 reaction center. FEBS Letters 205:82–86

Chang CH, El-Kabbani O, Tiede D, Norris J, Schiffer M (1991) Structure of the membrane bound protein photosynthetic reaction center from *Rhodobacter sphaeroides*. Biochemistry 30: 5352–5360

Chirino AJ, Lous EJ, Huber M, Allen JP, Schenck CC, Paddock ML, Feher G, Rees D (1994) Crystallographic analyses of site-directed mutants of the photosynthetic reaction center from *Rhodobacter sphaeroides*. Biochemistry 33:4584–4593

De Groot HJ, Gebhard R, Vanderhoef I, Hoff AJ, Lugtenburg J, Violette CA, Frank HA (1992) C-magic angle spinning NMR evidence for a 15.15′-cis configuration of the spheroidene in the *Rhodobacter sphaeroides* photosynthetic reaction center. Biochemistry 31:12446–12450

Deisenhofer J, Michel H (1989) The photosynthetic reaction centre from the purple bacterium *Rhodospeudomonas viridis*. Embo J 8:2149–2170

Deisenhofer J, Epp O, Miki K, Huber R, Michel H (1984) X ray structure analysis of a membrane protein complex. Electron density map at 3 Å resolution and a model of the chromophores of the photosynthetic reaction center from *Rhodopseudomonas viridis*. J Mol Biol 180:385–398

Deisenhofer J, Epp O, Miki K, Huber R, Michel H (1985) Structure of the protein subunits in the photosynthetic reaction centre of *Rhodopseudomonas viridis* at 3 Å resolution. Nature 318:618–624

Deisenhofer J, Epp O, Sinning I, Michel H (1995) Crystallographic refinement at 2.3 Å resolution and refined model of the photosynthetic reaction centre from *Rhodopseudomonas viridis*. J Mol Biol 246:429–457

Ducruix A, Reiss-Husson F (1987) Preliminary characterization by X-ray diffraction of crystals of photochemical reaction centres from wild-type *Rhodopseudomonas sphaeroides*. J Mol Biol 193:419–421

El-Kabbani O, Chang CH, Tiede D, Norris J, Schiffer M (1991) Comparison of reaction centers from *Rhodobacter sphaeroides* and *Rhodopseudomonas viridis*. Overall architecture and protein-pigment interactions. Biochemistry 30:5361–5369

Ermler U, Fritzsch G, Buchanan SK, Michel H (1994) Structure of the photosynthetic reaction centre from *Rhodobacter sphaeroides* at 2.65 Å resolution: cofactors and protein-cofactor interactions. Structure 2:925–936

Gunner MR (1991) The reaction center protein from purple bacteria. Structure and function. In: Lee CP (ed) Current Topics in Bioenergetics, vol 16. Academic Press, New York, pp 319–367

Komiya H, Yeates TO, Rees DC, Allen JP, Feher G (1988) Structure of the reaction center from *Rhodobacter sphaeroides* R-26 and 2.4.1.: symmetry relations and sequence comparisons between different species. Proc Natl Acad Sci USA 85:9012–9016

Paddock ML, Rongey SH, Feher G, Okamura MY (1989) Pathway of proton transfer in bacterial reaction centers. Replacement of glutamic acid 212 in the L-subunit by glutamine inhibits quinone (secondary acceptor) turnover. Proc Natl Acad Sci USA 86: 6602–6606

Paddock ML, McPherson PH, Feher G, Okamura MY (1990) Pathway of proton transfer in bacterial reaction centers. Replacement of serine-L223 by alanine inhibits electron and proton transfers associated with reduction of quinone to dihydroquinone. Proc Natl Acad Sci USA 87:6803–6807

Reiss-Husson F, Arnoux B, Ducruix A, Steck K, Mäntele W, Schiffer M, Chang CH (1990) Spectroscopic and structural studies of crystallized reaction centres from wild type *Rhodobacter sphaeroides* Y. In: Drews G and Dawes EA (eds) Molecular Biology of Membrane-Bound Complexes in Phototrophic Bacteria. Plenum Press, New York, pp. 323–328

Roth M, Lewit-Bentley A, Michel H, Deisenhofer J, Huber R, Oesterhelt D (1989) Detergent structure in crystals of a bacterial photosynthetic reaction centre. Nature 340:659–662

Roth M, Arnoux B, Ducruix R, Reiss-Husson F (1991) Structure of the detergent phase and protein-detergent interactions in crystals of the wild-type (strain-Y) *Rhodobacter sphaeroides* photochemical reaction center. Biochemistry 30:9403–9413

Sheldrick GM (1993) SHELXL93, Program for the Refinement of Crystal Structures. University of Göttingen, Germany

Sousa R, Lafer EM, Wang BC (1991) Preparation of crystals of T7 RNA polymerase suitable for high-resolution X-ray structure analysis. J Crystal Growth 110:237–246

Stilz HU, Finkele U, Holzapfel W, Lauterwasser C, Zinth W, Oesterhelt D (1994) Influence of M subunit Thr222 and Trp252 on quinone binding and electron transfer in *Rhodobacter sphaeroides* reaction centres. Eur J Biochem 223:233–242

Tronrud DE, Schmid MF, Matthews BW (1986) Structure and X-ray amino acid sequence of a bacteriochlorophyll a protein from *Prosthecochloris aestuarii* refined at 1.9 Å resolution. J Mol Biol 188:443–454

Warncke K, Gunner MR, Braun BS, Gu L, Yu CA, Bruce JM, Dutton PL (1994) Influence of hydrocarbon tail structure on quinone binding and electron-transfer performance at the Q_A and Q_B sites of the photosynthetic reaction center protein. Biochemistry 33:7830–7841

Yeates TO, Komiya H, Chirino A, Rees D, Allen JP, Feher G (1988) Structure of the reaction center from *Rhodobacter sphaeroides* R26 and 2.4.1.: protein-cofactor (bacteriochlorophyll, bacteriopheophytin, and carotenoid) interactions. Proc Natl Acad Sci USA 85:7993–7997